Superconductivity 8 (2023) 100066

Contents lists available at ScienceDirect

Superconductivity

journal homepage: www.elsevier.com/locate/supcon

Full Length Article

Time-dependent development of dynamic resistance voltage of superconducting tape considering heat accumulation

Chao Li [a], Yuying Xing [b,*], Ying Xin [a], Bin Li [a], Francesco Grilli [c]

[a] Tianjin University, School of Electrical and Information Engineering, Tianjin, China
[b] State Grid Tianjin Electric Power Company Chengnan Power Supply Branch, Tianjin, China
[c] Karlsruhe Institute of Technology, Institute for Technical Physics, Karlsruhe, Germany

ARTICLE INFO

Keywords:
Dynamic resistance
High temperature superconductor
Electromagnetic-thermal coupling
Finite element method
REBCO coated conductors

ABSTRACT

In flux pumps, motors and superconducting magnets, the high temperature superconductor (HTS) coated conductor frequently carries a DC transport current when an oscillating magnetic field is present in the background. Under this circumstance, the interesting effect of dynamic resistance takes place, which can affect the operating performance of superconducting devices: heat accumulation can contribute to the rising temperature of the HTS tape and the dynamic resistance voltage can change accordingly. This article explores the time-dependent development of the dynamic resistance voltage using a numerical modeling considering the thermal effects. After a validation against experimental results, this work investigates the effects of several factors on the structure of the HTS tape on the time-dependent development of the dynamic resistance, thus providing insights toward a better understanding of the time-dependent behavior of HTS tapes under external magnetic fields.

1. Introduction

HTS coated conductor is extensively used in superconducting magnets [1], fault current limiters [2] and motors [3] due to their superior current-carrying capacity, field performance and mechanical durability. Under the applications mentioned above, it is typical that HTS coated conductors carry DC transport currents when there is a background magnetic fields present [4,5]. The dynamic resistance effect–i.e., in this case, a DC voltage is generated in the direction of the DC transport current. This effect has important practical consequences for HTS applications: on the one hand, the dynamic resistance contributes to the power dissipation, which impacts the efficiency of superconducting devices [6,7]; on the other hand, it has a significant impact on the applications such as field-controlled persistent current switches for superconducting magnets or flux pumps, which are capable of wirelessly energizing closed superconducting coils [8–11].

Several investigations on the dynamic resistance have already been carried out, and a brief summary is presented here. Analytical models based on the critical state model calculating the dynamic resistance in an HTS tape have been proposed in [12–14]. Oomen explained the generation of dynamic resistance and proposed a mathematical model for calculating it in the superconducting slab [15]. Ciszek *et al.* investigated the relationship between dynamic resistance losses and the DC transport current as well as the dynamic resistance's angular field dependence [16]. Jiang *et al.* conducted several experiments and studies to determine the dynamic resistance and revealed its function in flux pumping phenomena [17,18]. Ainslie *et al.* proposed numerical models to study the characteristics of the dynamic resistance [19,20]. Ma *et al.* developed a temperature-dependent multilayer model to investigate how temperature affects HTS tapes [21,22]. The transient waveforms of dynamic resistance with different HTS tapes and their relation to the J_c-(B, θ) dependence were shown in [23,24]. Li *et al.* proposed a technique to monitor the condition of DC-carrying HTS tapes exposed to an AC magnetic field by using the ratio of the DC component to the second harmonic component of the voltage response [25,26]. A full-range formulation using the binomial theorem and Euler's formula for calculating the dissipative loss originating from the dynamic resistance was proposed in [27,28]. Besides, researches on dynamic resistance have been extended to stacks of tapes connected in series and parallel [29–31]. The voltage drop along a superconducting loop, rather than an HTS tape, carrying DC current under a perpendicular oscillating field was investigated in [32].

Most previous analyses and numerical models focused on the dynamic resistance under low field or low frequency in ideal cases,

* Corresponding author.
E-mail addresses: yuy_xing@163.com (Y. Xing), francesco.grilli@kit.edu (F. Grilli).

https://doi.org/10.1016/j.supcon.2023.100066
Received 24 April 2023; Revised 11 September 2023; Accepted 14 September 2023
Available online 20 September 2023

assuming that the HTS tapes' normal operating temperature of 77 K remains constant. However, in real application when the applied AC magnetic field is relatively strong or the DC transport current approaches the HTS tapes' critical current, the inability of a significant quantity of Joule heat to disperse in a timely manner causes the temperature of HTS tapes to increase [33]. Correspondingly, over numerous AC cycles, the dynamic resistance voltage will be significantly affected and this change aggravates the situation through generating more Joule heat. The phenomenon has been reported in recent experimental measurements [34]. Hence, in order to accurately illustrate the complex and dynamic voltage response of the HTS tape carrying DC currents while subjected to the background of AC magnetic field and assess the performance of superconducting devices involving dynamic resistance, it is necessary to consider how the dynamic resistance voltage changes over time on HTS tapes. It is also necessary to take into account how electromagnetic-thermal coupling affects the dynamic resistance voltage, but there is still a lack of comprehensive researches on this aspect [35].

In this article, the dynamic resistance voltage's temporally dependent developments were explored using an electromagnetic-thermal coupling model, which were verified by experimental tests. Factors such as the structure of the HTS tape and the heat accumulation, which can impact the dynamic resistance voltage's temporally dependent development, were investigated. Finally, the recovery of dynamic resistance voltage in various cases was researched.

2. Dynamic resistance voltage and modelling methodology

2.1. Origin of the dynamic resistance voltage

Dynamic resistance voltage is the result of periodic magnetic flux mobility that is sparked by an external AC magnetic field that is applied to an HTS tape carrying a DC transport current. If the applied magnetic field is less than a particular threshold field $B_{a,th}$, no net flux may traverse the HTS tape, and no dynamic resistance voltage occurs, as shown in Fig. 1(a) and (b). As illustrated in Fig. 1(c) and (d), the HTS tape experiences some magnetic flux that enters from one side and escapes from the other when the applied magnetic field is greater than the threshold field $B_{a,th}$. Due to the flux motion traversing the central region where the DC transport current flows, a DC voltage is generated along the same direction of the DC current, which is the dynamic resistance effect.

2.2. Electromagnetic-thermal coupling model

Using the finite element technique (FEM) based on the H formulation, a 2D numerical model taking into account electromagnetic and thermal coupling was constructed to evaluate the time evolution of the current distribution and the magnetic field within an HTS tape [36]. The model was implemented in the FEM program COMSOL Multiphysics.

The three-layer construction of the multi-layer HTS tape is depicted in Fig. 2(a), with the superconducting layer sandwiched between two copper layers that act as stabilizers. Nearly all of the DC transport current is dispersed either in the superconducting layer or the copper layers, beacuse the resistivity of the substrate layer is significantly higher than that of the copper layers [30]. Hence, the substrate layer is ignored to simplify the model and accelerate calculations. And the superconducting layer and the copper layers are electrically connected in parallel as shown in Fig. 2(b). While an external AC magnetic field is supplied perpendicular to the HTS tape along the *y*-axis, DC transport current flows in the HTS tape along the *z*-axis.

The electromagnetic and thermal modules are coupled in the numerical model. The electromagnetic module's governing equations are as follows:

$$\nabla \times E = -\mu_0 \cdot \partial H/\partial t, \qquad \nabla \times H = J, \tag{1}$$

where $\mu_0 = 4\pi \times 10^{-7}$H/m is the permeability of free space.

The electrical behaviour of the HTS tape is described by an *E-J* power law:

$$E = E_0 \cdot (J/J_c(B,T))^n, \tag{2}$$

where n is the power index and E_0 is standard electric field criterion, $J_c(B, T)$ is the critical current density, which depends on the magnetic field and the temperature.

The thermal module relies on the heat transfer equation to calculate the real-time temperature of the HTS tape:

$$\rho C_p \cdot \partial T/\partial t - \nabla \cdot (k\nabla T) = Q - q_0, \tag{3}$$

where ρ is the mass density, C_p is the heat capacity, k is the thermal conductivity, The data for these parameters are obtained from [37,38]. Q is the internal heat source produced by the HTS tape and q_0 is the convective heat flow between the surrounding liquid nitrogen and the HTS tape:

$$Q = \int qds = \int E \cdot Jds, \qquad q_0 = h \cdot (T_{ext} - T), \tag{4}$$

where h is the heat transfer coefficient according to the experiment tests presented in [22], T is the actual temperature of the HTS tape, and T_{ext} is the ambient temperature.

The coupling between two modules is realized through the relationship between the internal heat Q and the temperature T as shown in Fig. 3. In this way, two modules work together to present the time-dependent develoment of the dynamic resistance voltage in a more practical way.

3. Investigation on time-dependent development of dynamic resistance voltage

3.1. Time-dependent development of dynamic resistance voltage and experimental verification

To confirm the validity of the proposed numerical model, the dynamic resistance voltage measured by experimental tests, calculated by numerical models with and without thermal coupling, are compared in Fig. 4. A quick review of the HTS tape's specifications is provided in Table 1.

The average dynamic resistance voltage of the HTS tape under various DC transport currents is depicted in Fig. 4(a) and (b). In Fig. 4(a) and (b), the applied magnetic field has a frequency of 50 Hz and 200 Hz, respectively. The experimental curves are plotted in green dot line; the simulation results without thermal coupling in blue; the simulation results with thermal coupling in red. The triangle and circle shaped curves show the 60 and 100 mT applied magnetic field strengths, respectively. When the DC transport current, magnetic field strength, and frequency are relatively low, the dynamic resistance curves of the HTS tape with and without thermal coupling match the measured dynamic resistance curves well. However, when the frequency or strength of the magnetic field becomes large or the transport current approaches the critical current, the simulation results with thermal coupling are closer to the experimental data.

Fig. 4(c) - (h) show the instantaneous waveforms of the dynamic resistance voltage corresponding to the points surrounded by black and orange dashed-line boxes in Fig. 4(b). Using the same color scheme described above, Fig. 4(c) and (f) represent the experimental results, Fig. 4(d) and (g) represent the dynamic resistance voltage calculated without thermal coupling, Fig. 4(e) and (h) represent the dynamic resistance voltage calculated with thermal coupling. As shown in Fig. 4(c) and (f), the measured dynamic resistance voltage waveforms show time-dependent characteristics: the dynamic resis-

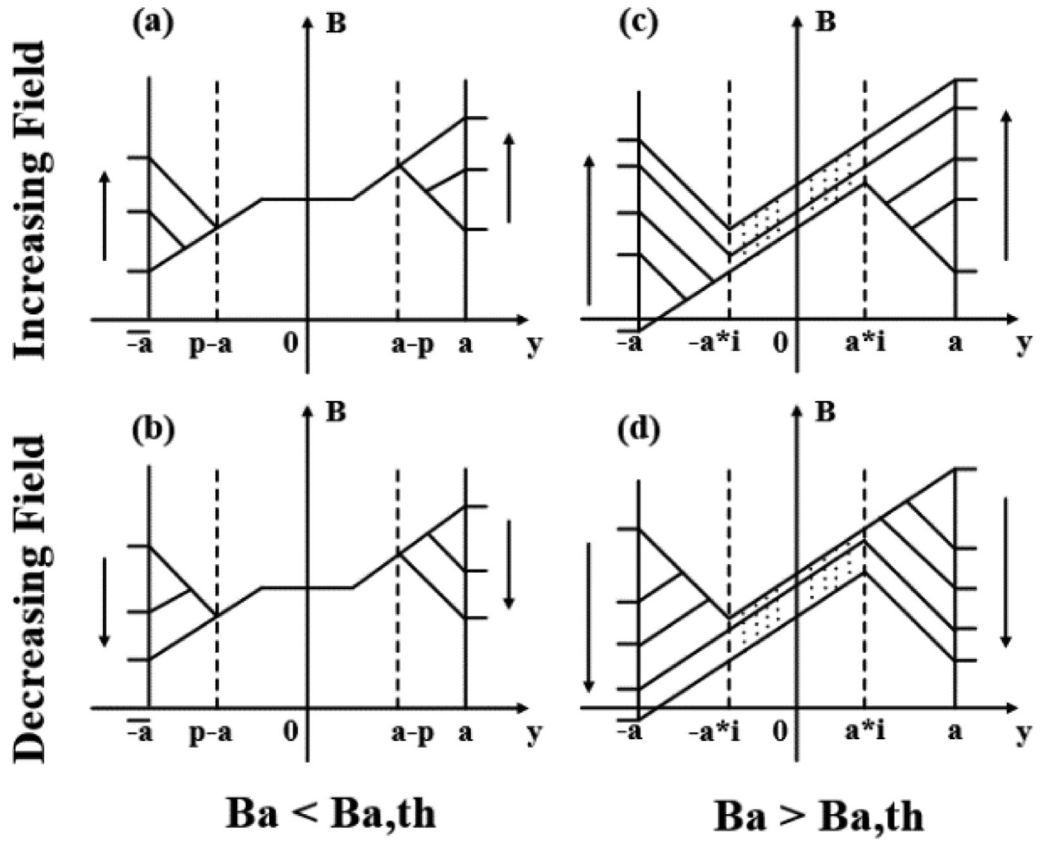

Fig. 1. Field profile inside the HTS slab [26], where "a" represents the half width of the HTS slab, "p" represents the penetration depth of the magnetic field in the HTS slab, "B_a"represents the amplitude of the external magnetic field and "$B_{a,th}$" represents a specific threshold field of the HTS slab.

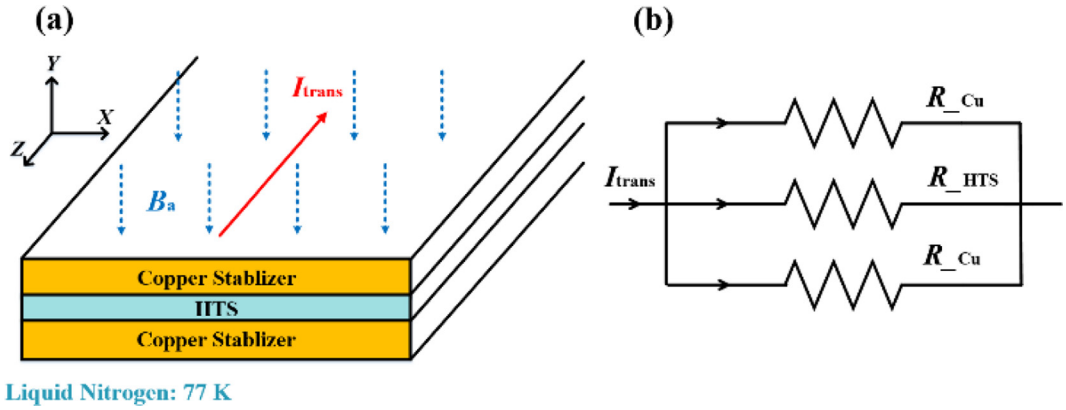

Fig. 2. (a) Schematic drawing of HTS tape with multi-layer structure under AC magnetic field, where "B_a"is the the amplitude of the external magnetic field, I_{trans} is the DC transport current. (b) Diagram of electrical equivalents of the superconducting layer and copper layers, where $R_{\_layer}$ resprsents the resistance of each layer.

tance voltage keeps rising over time. The higher the transport current flowing in the HTS tape, the more obvious the increasing trend of the dynamic resistance voltage. However, such a time-dependent rise is not reflected in the dynamic resistance voltage curves estimated by models without thermal coupling.

The observed increase of dynamic resistance voltage with time can be explained as follows. The HTS tape mainly contains three layers, where the superconducting layer is sandwiched with two copper stabilizer layers. The three layers are connected in parallel from the perspective of an electrical circuit, as shown in Fig. 2(b). The resistance of the copper layers can be regarded as constant, so the overall resistance of the entire HTS tape changes in response to changes in the dynamic resistance of the superconducting layer. When the DC transport current is relatively large, the HTS tape's temperature is growing because the Joule heat produced in it cannot be dispersed over time. Additionally, the temperature increase also has a significant effect on the HTS tape's dynamic resistance.

Additionally, it should be noticed that as the dynamic resistance rises, the distribution of the DC transport current within HTS tape alters. In Fig. 5(a) and (b), the DC transport current in the superconducting layer and the copper layer are depicted by the red curves I_{sc} and green curves I_{Cu}, respectively. The temperature is not uniform in

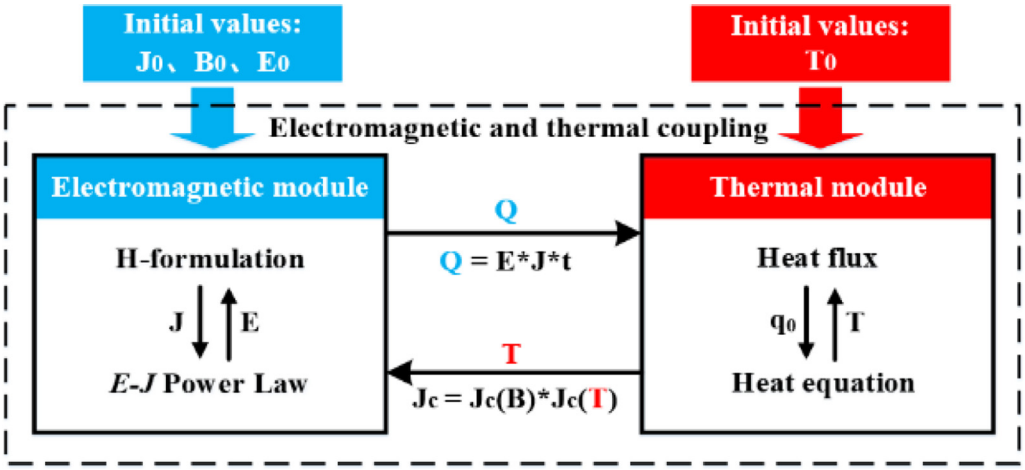

Fig. 3. Flowchart of the calculation of the dynamic resistance voltage of an HTS tape considering thermal coupling.

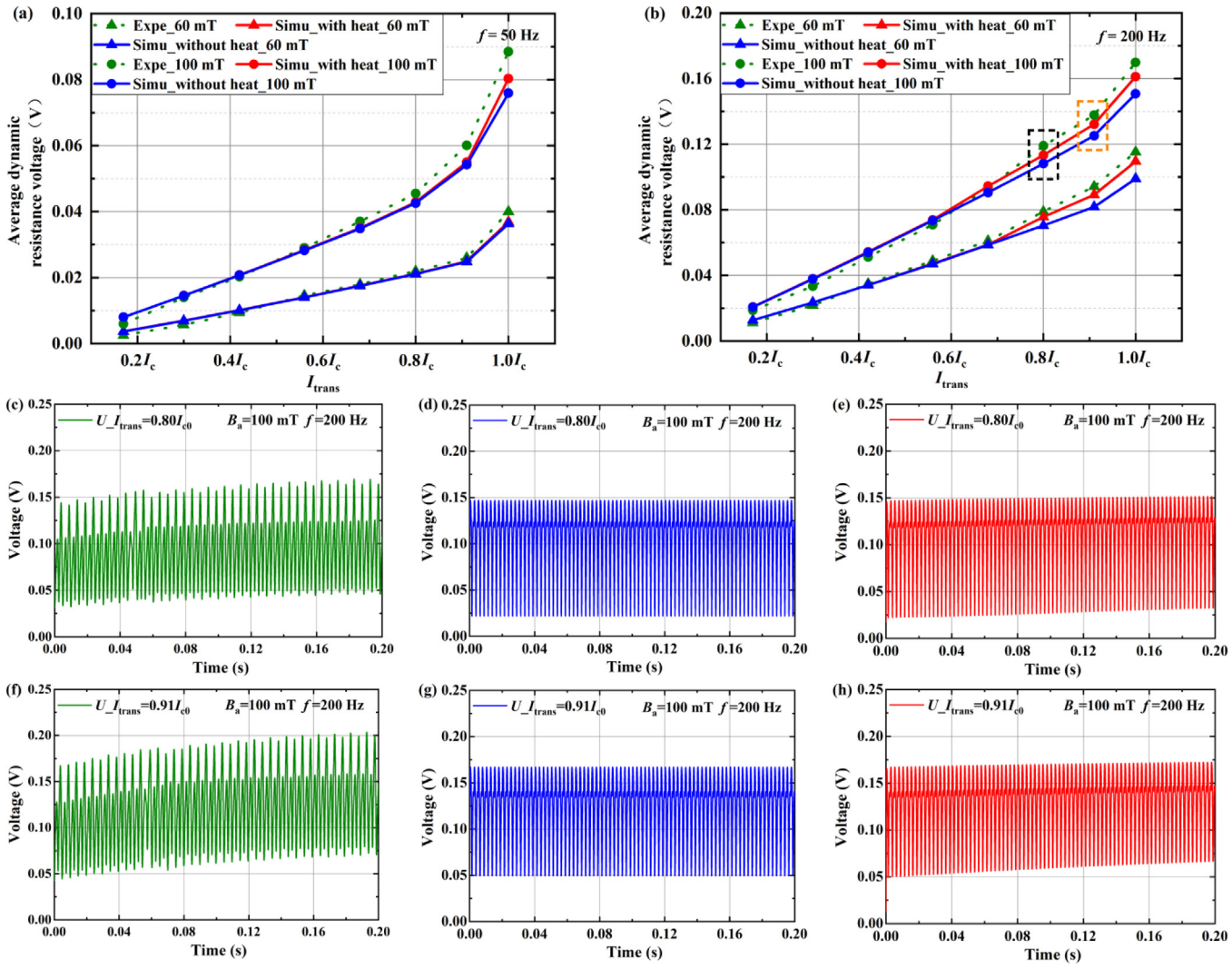

Fig. 4. Dynamic resistance voltage under 60, 100 mT and 50 Hz, 200 Hz for I_{trans} = 0.17, 0.30, 0.42, 0.56, 0.68, 0.80, 0.91,1.00I_{c0}, where I_{c0} is the critical current of HTS tape at 77 K; (a), (b) show the average dynamic resistance; (c)-(h) are instantaneous waveforms corresponding to the points surrounded by dashed lines in (b), which the magnetic field is 100 mT, 200 Hz and I_{trans} = 0.8I_{c0}, 0.91I_{c0}; (c), (f) are obtained through experiment; (d), (g) are obtained through non-thermal coupling model; (e), (h) are obtained through thermal coupling model.

Table 1
Characteristics of the HTS tape.

Parameters	Value	Parameters	Value
HTS width	6 mm	Cu layers thickness	20 μm
E_0	10^{-4} V/m	HTS layer thickness	1 μm
n	21	h	800 W/ m^2·K
I_{c0} at 77 K	86 A	C_p (ReBCO)	(100–140) J/kg·K
T_{ext}	77 K	k (ReBCO)	(8–12) W/m·K
T_0	77 K	ρ (ReBCO)	5900 kg/m^3
T_c	92 K	C_p (Cu)	(180–220) J/kg·K
ρ (Cu)	8000 kg/m^3	k (Cu)	(500–700) W/m·K

the HTS tape: as a simplification, the HTS tape's core region is chosen to reflect the tape's total temperature. As can be observed, increasing transport current causes the HTS tape to heat up and causes more transport current to flow from the superconducting layer into the copper layers.

No matter how large the DC transport is, the dynamic resistance is always constant in the model without thermal coupling, which disregards the impact of temperature, as shown in Fig. 5(c). Under this circumstance, the transport current distribution does not change. Therefore, to accurately depict the development of the dynamic resistance's trend, the temperature of HTS tapes with time must be considered.

3.2. Impact of varying-thickness copper layers on the temperature when the magnetic field is low

The dynamic resistance and temperature development of the HTS tape are impacted by the copper layer. The dynamic resistance of

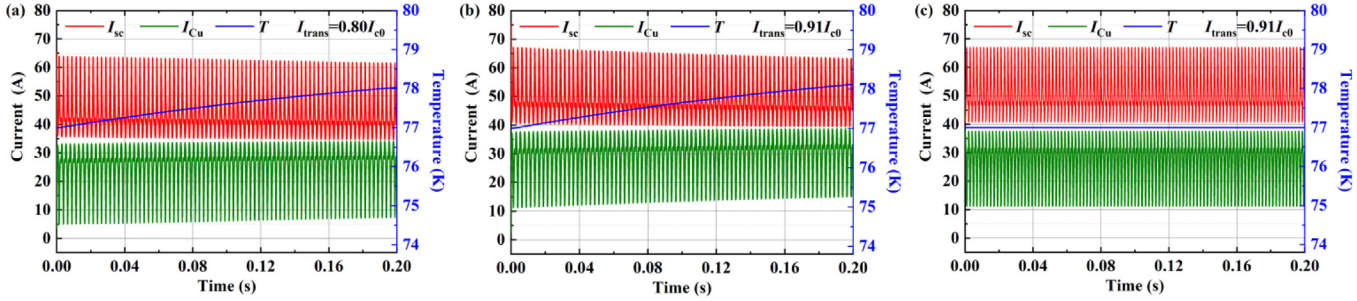

Fig. 5. Time-dependent distribution of DC transport current flowing into the HTS layer, copper layer and the temperature of the central area of the HTS tape when the magnetic field is 100 mT, 200 Hz; (a) is obtained through thermal coupling model when $I_{trans} = 0.8I_{c0}$, (b) is obtained through thermal coupling model when $I_{trans} = 0.91I_{c0}$, (c) is obtained through non-thermal coupling model when $I_{trans} = 0.91I_{c0}$.

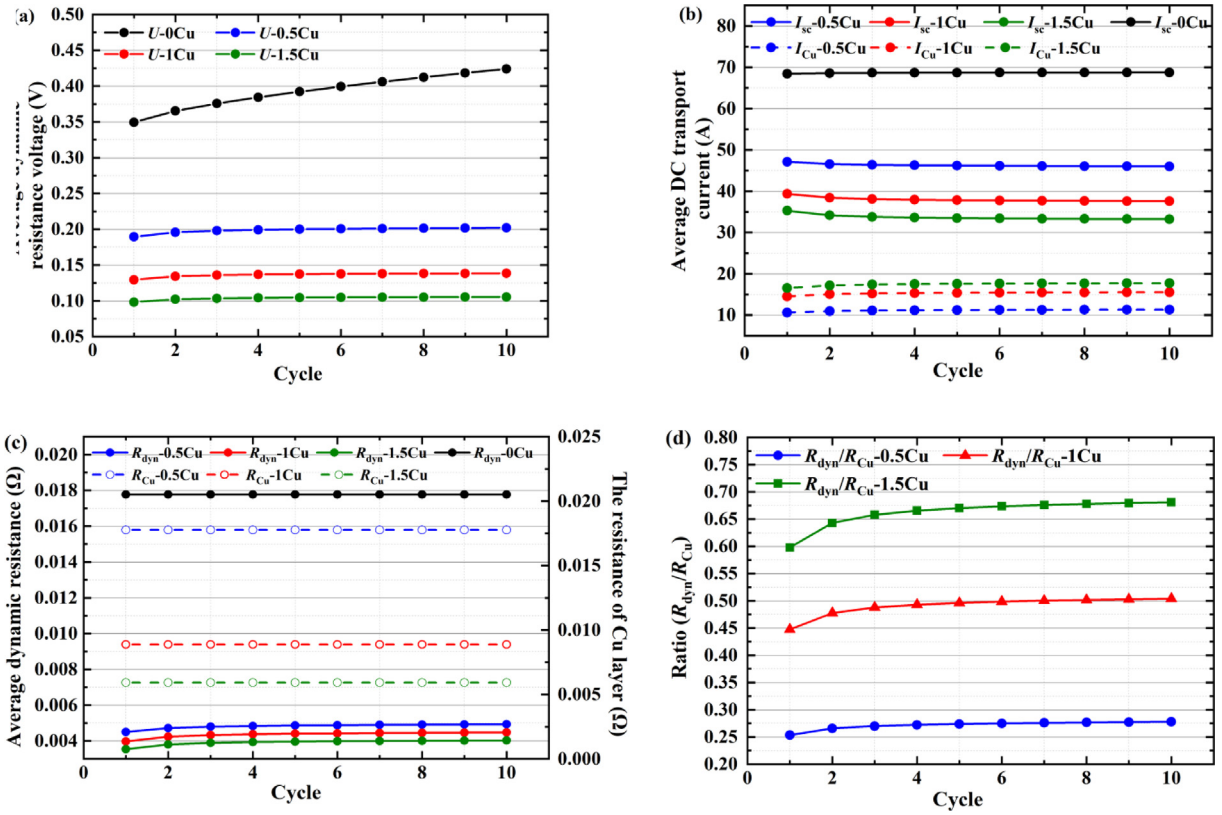

Fig. 6. Influence of varying-thickness copper layers when the applied AC magnetic field is 50 mT, 1000 Hz and $I_{trans} = 0.8I_{c0}$; (a) shows the average dynamic resistance voltage, (b) shows the distribution of the transport current, (c) shows the dynamic resistance and (d) shows the ratio of the dynamic resistance of the HTS tape to the resistance of the copper layer. All the simulations were performed with the electromagnetic-thermal coupled model.

the HTS tape with copper layers of different thicknesses is simulated and evaluated in the sections that follow.

To demonstrate how the dynamic resistance characteristics of HTS tape change over time when considering thermal coupling, this article selected a period of time to explain. The average dynamic resistance voltage, the transport current distribution and the average dynamic resistance of the HTS tape are shown in Fig. 6. The copper layers thicknesses are selected as 0, 0.5, 1, and 1.5 times the normal thickness (20 μm) of the copper layer. The applied AC magnetic field is 50 mT at 1000 Hz. To prevent quenching of the HTS tape, the DC transport current is set at $0.8I_{c0}$, and the *x*-axis "Cycle" represents the period of the applied AC magnetic field.

It can be seen from Fig. 6(a) that the dynamic resistance voltage increases with decreasing thickness of the copper layers. The resistance of the superconducting layer and copper layers both rise with decreasing copper layer thickness because of the parallel connection between the copper layers and the superconducting layer (Fig. 6(c)). However, the ratio of the dynamic resistance to the resistance of the copper layer decreases with the decreasing of copper layers thickness as shown in Fig. 6(d). Therefore, more transport current flows into the superconducting layer as shown in Fig. 6(b), which results in stronger magnetic flux motion inside the HTS tape, and larger dynamic resistance. The extreme case is the HTS tape without copper layers, which means that the copper layers thickness is reduced to zero. Then, the dynamic resistance voltage of the HTS tape is much larger than HTS tapes with copper layers. This is also because the DC transport current has no other path to flow but the superconducting layer.

Fig. 7 shows the distribution of the current density in the superconducting layer with (Fig. 7(a)) and without copper layers (Fig. 7(b)) in the 2nd and 10th period of applied AC magnetic field.

The distributions are displayed at the negative and the positive peaks of the 50 mT, 1000 Hz applied magnetic field.

When the DC transport current is $0.8I_{c0}$, the curves of the distribution of the current density in the superconducting layer with copper layers are overlapped in different cycles as shown in Fig. 7(a); whereas the current density distribution in the superconducting layer without copper layers obviously develops with time as shown in Fig. 7(b). After 10 cycles of the applied field, the distribution of the current density nearly occupies the entire superconducting layer, which means that the central region where the flux motion travers and the DC transport current flows has expanded to the entire HTS layer.

The temperature rises fast only in the HTS tape without copper layers compared with the temperature of HTS tapes with copper layers in Fig. 8. The temperature difference is consistent with the dynamic resistance voltage curves shown in Fig. 6(a). Within the same time interval, HTS tapes with copper layers exhibit a smaller temperature increase, while the HTS tape without copper layers experiences a higher and more pronounced temperature rise.

3.3. Impact of varying-thickness copper layers on the temperature when the magnetic field is high

The analysis in the previous section shows that the thickness of the copper layers has little effect on the dynamic resistance of the HTS tape with copper layers when the applied magnetic field is low. However, when it comes to higher AC magnetic field, things are different. In the following, a 'high' magnetic field of 200 mT and 1000 Hz is applied to compare HTS tapes' dynamic resistance voltage with varying-thickness copper layers.

The dynamic resistance voltage, the DC transport current distribution within the HTS tape, the dynamic resistance, and the ratio of the HTS tape's dynamic resistance to the resistance of the copper layer with variable thickness are all displayed in Fig. 9. Compared with the curves in Fig. 6, the dynamic resistance voltages in Fig. 9(a) significantly increase under the high applied field, and the current flowing into the copper layer is even larger than that flowing in the superconducting layer as shown in Fig. 9(b).

This is because the dynamic resistance of the HTS layer has exceeded the resistance of the copper layer, as shown in Fig. 9(c)

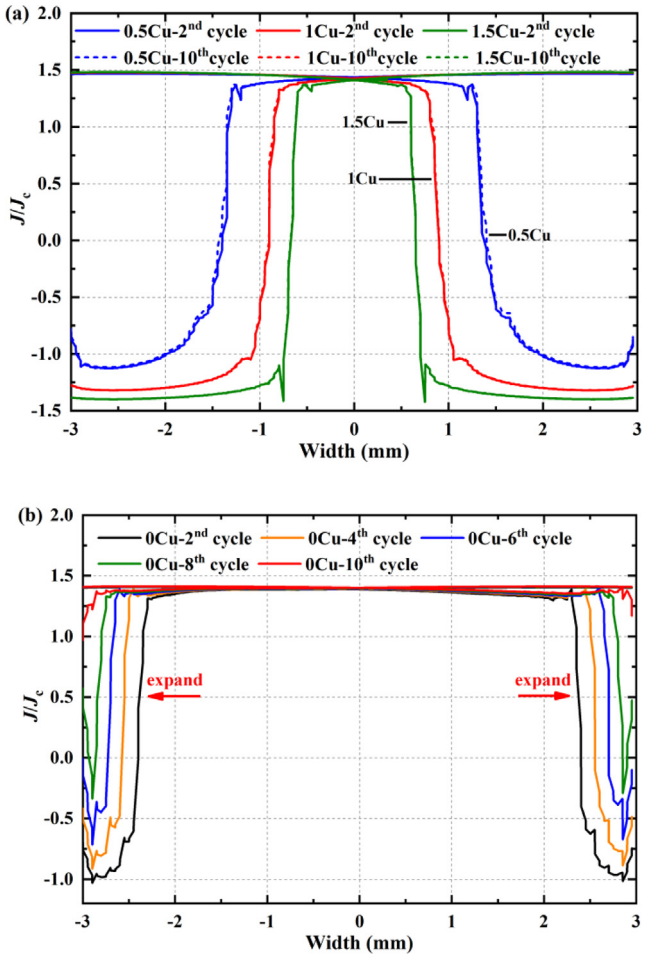

Fig. 7. Curves of the current density distribution in superconducting layer in different cycles of 50 mT and 1000 Hz applied magnetic field; (a) with 0.5, 1, 1.5 times the normal copper layer thickness; (b) without copper layers.

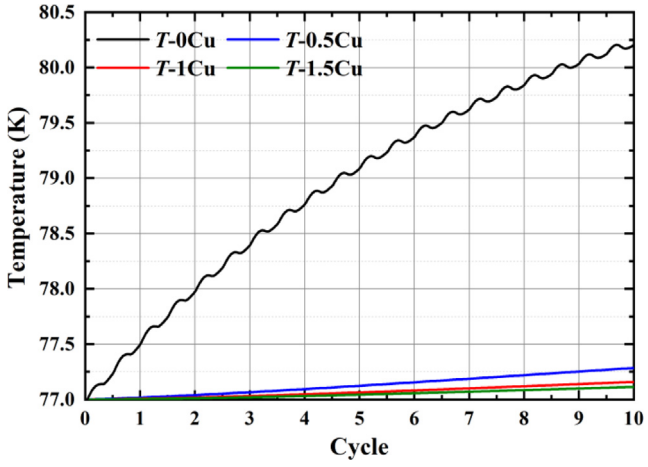

Fig. 8. Temperature of the central area of the HTS tape under varying-thickness copper layers when the magnetic field is 50 mT, 1000 Hz and the DC transport current is $0.8I_{c0}$.

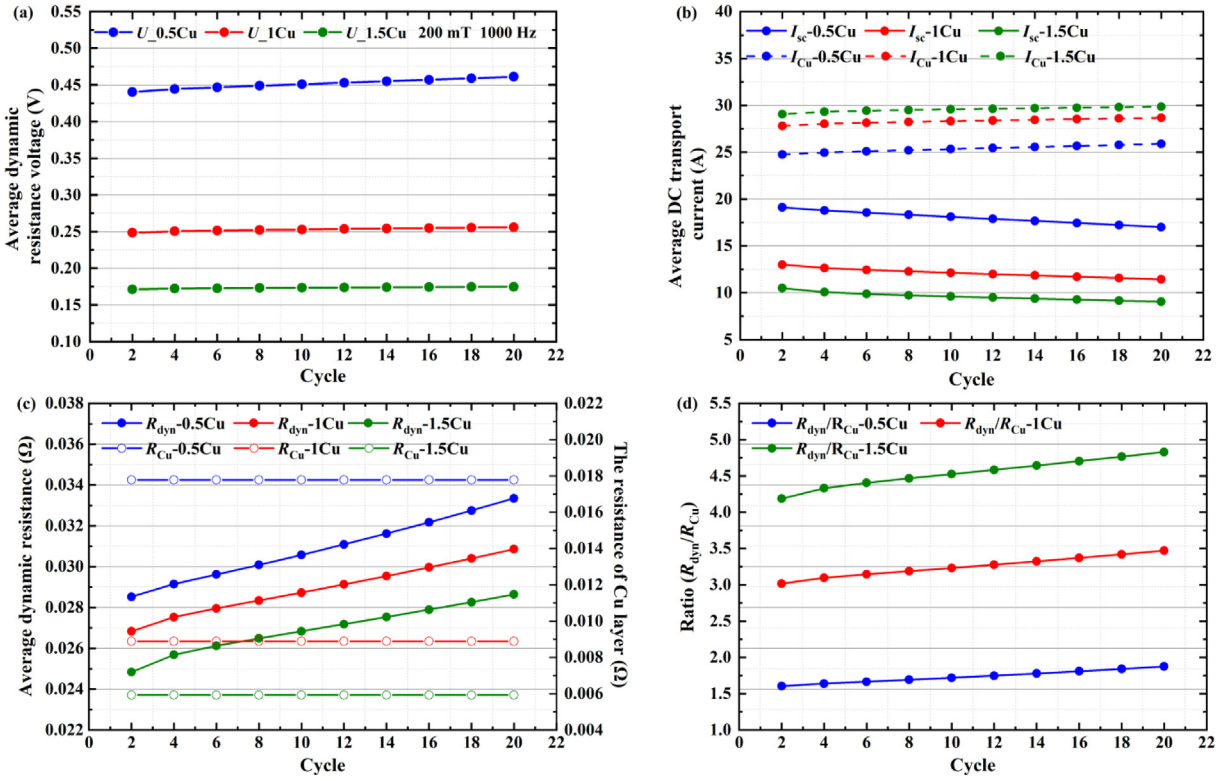

Fig. 9. Calculated by the thermal coupling model under varying-thickness copper layers when the applied AC magnetic field is 200 mT, 1000 Hz and $I_{trans} = 0.8I_{c0}$; (a) shows the average dynamic resistance voltage, (b) shows the distribution of the transport current, (c) shows the dynamic resistance and (d) shows the ratio of the dynamic resistance of the HTS tape to the resistance of the copper layer.

and (d). Additionally, it is evident that when the thickness of the copper layers decreases, the dynamic resistance voltage and the current flowing into the superconducting layer both rise. Additionally, the time-dependent increase of dynamic resistance voltage is more visible the thinner the copper layers are.

The current density distribution in superconducting layer under varying-thickness copper layers shown in Fig. 10 are obtained at the negative and the positive peaks of the 2nd and 20th period of the applied magnetic field, where cycle means the period of the magnetic field. The smaller copper layers thickness, the larger the area of the central region of the HTS tape where the flux motion travers and the DC transport current flows. Compared with that in the 2nd cycle, the area of the central region in the 20th cycle develops larger. The developed area is negatively related with the copper layers thickness. The phenomenon is caused by the net Joule heat accumulating discussed in the following.

The temperature change of the HTS tape is not large, so the heat capacity of each material changes relatively little. For the convenience of analysis, the heat capacities were assumed to be constant. Thus, the

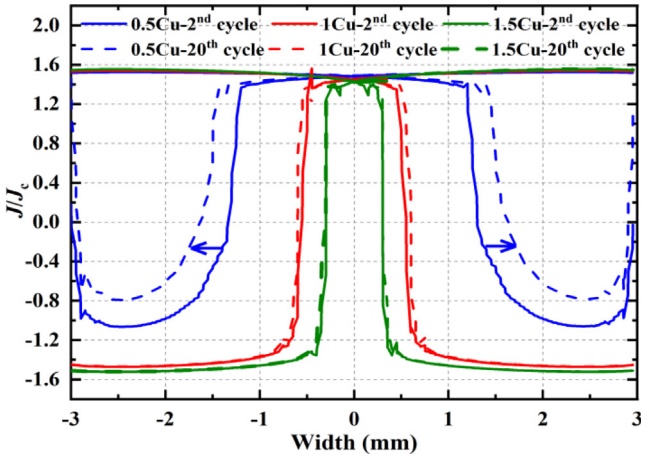

Fig. 10. Curves of the current density distribution in superconducting layer in the 2nd and 20th cycle of 200mT and 1000 Hz applied magnetic field of 0.5, 1, 1.5 times the normal copper layer thickness.

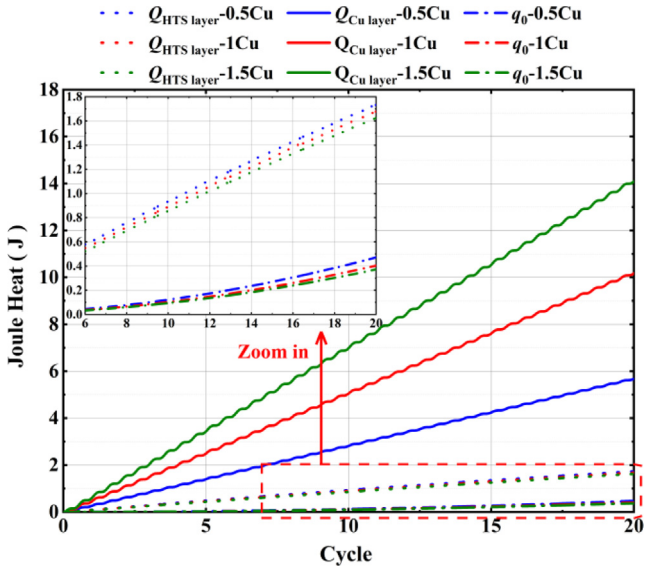

Fig. 11. Curves of Joule heat generation of different layers and the overall heat dissipation of the HTS tape under varying-thickness copper layers.

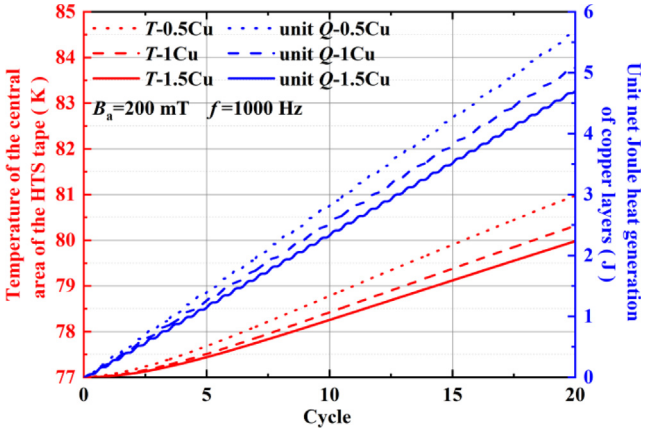

Fig. 12. Curves of the unit net Joule heat generation and the temperature of the HTS tape of 0.5, 1, 1.5 times the normal copper layer thickness.

temperature of the HTS tape is determined by the net Joule heat $Q_{\text{Net heat}}$, which is the difference between the heat generation and the heat dissipation that changes the temperature of the HTS tape. According to equations (3) and (4), we can get,

$$Q_{\text{Net heat}} = Q_{\text{sc}} + Q_{\text{copper}} - q_0 \quad , \tag{5}$$

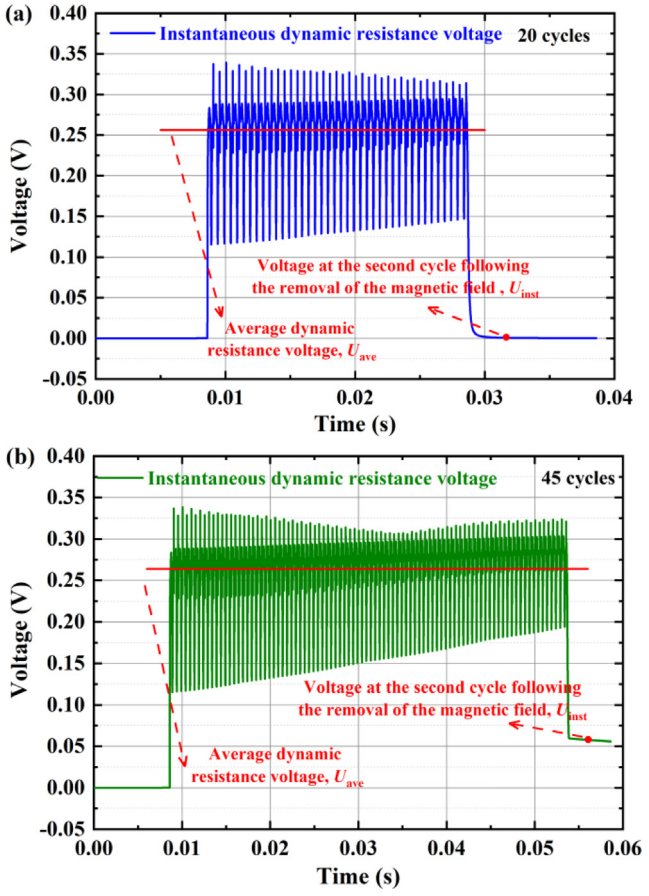

Fig. 13. Instantaneous dynamic resistance voltage of the HTS tape carrying DC transport current of $0.8I_{c0}$ under the applied AC magnetic field of 200 mT, 1000 Hz; (a) shows the dynamic resistance voltage for 20 cycles of the applied field, and (b) shows the dynamic resistance voltage for 45 cycles of the applied field.

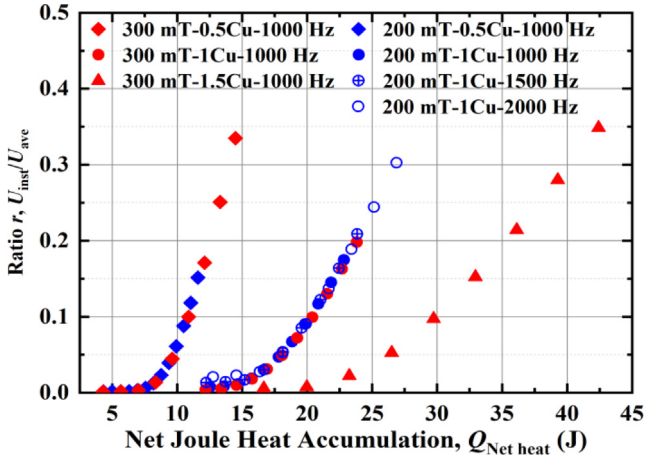

Fig. 14. The ratio r of the recovery voltage to the average dynamic resistance voltage for different cycles under different magnetic field and varying-thickness copper layers.

where Q_{sc} and Q_{copper} represent the Joule heat generated in the superconducting layer and copper layers respectively, and q_0 represents the heat dissipation of the HTS tape.

Fig. 11 shows the Joule heat generated in each layer of the HTS tape. It can be seen that the majority of the total Joule heat produced by the HTS tape is produced by heat generated in copper layers Q_{copper}, and Q_{copper} is positively correlated with copper layer thickness. This originates from more transport current flowing into copper layers. In addition, the heat dissipation is negatively related with the thickness of the copper layers. Hence, the temperature of the HTS tape with thicker copper layers should have been higher. However, the change of the temperature is opposite to what is expected, as shown in Fig. 12. This is because although more heat is accumulated by the thicker copper layers, the volume of copper layers is also larger. Correspondingly, the unit net Joule heat generation (net Joule heating generated by the HTS tape per unit length of 1 times the normal thickness of the copper layer) is reduced, and the temperature becomes lower. Besides, a lower temperature of the HTS tape also means less heat convection, so the heat dissipation is lower as well.

Therefore, it is the continuous increasing unit net Joule heat that leads to the increasing temperature of the HTS tape, which, then, also results in the increase with time of the central area of the region where the flux motion travers and the DC transport current flows. As a consequence, the dynamic resistance voltage presents a time-dependent development.

4. Recovery-voltage after removing the field

The part that follows looks at dynamic resistance voltage recovery. The real-time dynamic resistance voltage after applying the AC magnetic field of 200 mT, 1000 Hz for 20 cycles and 45 cycles is shown in Fig. 13. After 20 cycles, the dynamic resistance voltage can be swiftly brought back to zero when the magnetic field is turned off. In contrast, the dynamic resistance voltage delays the return to zero when the magnetic field is removed after 45 cycles.

In order to compare the recovery of the dynamic resistance voltage under different conditions, the ratio r of the instantaneous voltage to the average dynamic resistance voltage is selected as the criterion:

$$r = U_{\text{inst}}/U_{\text{ave}}. \tag{6}$$

The instantaneous voltage U_{inst} of the HTS tape in the second cycle following the removal of the magnetic field is represented by the marked red points in Fig. 13(a) and (b), and the average dynamic resis-

tance voltage U_{ave} of the HTS tape is represented by the marked red lines. Therefore, large ratio r indicates long recovery time of dynamic resistance voltage.

Fig. 14 shows the relation between the ratio r and the net Joule heat accumulated by the whole HTS tape under varying-thickness copper layers, varying frequencies and strengths of the magnetic field.

If the net Joule heat is the same, the ratio r of thin copper layers is larger than that of thick copper layers, for example, the larger the ratio r of the HTS tape when the value of x-axis in Fig. 14 is 15 J, it can be seen that the HTS tape with 0.5 times the thickness of the copper layers corresponds to a larger ratio r. According to equation (6) and Fig. 13, a larger ratio r results in a longer time required for the dynamic resistance voltage of the HTS tape to return to zero. If the copper layers thickness is constant, the curves of ratio r are overlapped, that is, the curves of the same thickness of the copper layers in Fig. 14 overlap into a curve under different magnetic field conditions.

This suggests the recovery time of the dynamic resistance voltage is determined by the net Joule heat and has nothing to do with the amplitude or frequency of the applied magnetic field. This finding can be useful for designing HTS tapes and superconducting devices.

5. Conclusion

This paper has concluded that it's the heat accumulation that results in the time-dependent behaviour of dynamic resistance voltage of superconducting tape. Experimental and simulation tests have been carried out to verify the analysis. Hence, it will be more accurate to consider the impacts of heat accumulation when the dynamic resistance voltage is relatively large.

The dynamic resistance voltage of the HTS tape with copper layers of different thickness is next investigated. The thickness of the copper layer has little bearing on the rate at which the dynamic resistance voltage develops under low field conditions. However, at high field conditions, thinner copper layers produce a more pronounced time-dependent dynamic resistance voltage growth. This is due to the fact that it is impossible to disregard the effect of the copper layer on the heat produced and dispersed by the HTS tape. Thinner copper layers result in more unit net Joule heat generated and higher temperature of the HTS tape.

Additionally, it has been discovered that the HTS tape's copper layers significantly affect how quickly the dynamic resistance voltage recovers. Long recovery times of the dynamic resistance voltage are necessary because to HTS tape's thin copper layer construction. The net Joule heat controls the dynamic resistance voltage recovery time when the thickness of the copper layers is constant.

Declaration of Competing Interest

The authors declare the following financial interests/personal relationships which may be considered as potential competing interests: Chao LI reports financial support was provided by The National Natural Science Foundation of China.

Acknowledgements

This research is partially funded by the National Natural Science Foundation of China (Grant No. 52107022).

References

[1] Hahn S et al. 45.5-tesla direct-current magnetic field generated with a high-temperature superconducting magnet. Nature 2019;570(7762):496–9 [Young-Gyun K, Seungyong H, Kwang Lok K, Oh Jun K, Haigun L. Investigation of HTS racetrack coil without turn-to-turn insulation for superconducting rotating machines. IEEE Trans Appl Supercond 2012;22(3):5200604].
[2] Shen B et al. Investigation on power dissipation in the saturated iron-core superconducting fault current limiter. IEEE Trans Appl Supercond 2019;29(2):1–5.
[3] Young-Gyun K, Seungyong H, Kwang Lok K, Oh Jun K, Haigun L. Investigation of HTS racetrack coil without turn-to-turn insulation for superconducting rotating machines. IEEE Trans Appl Supercond 2012;22(3):5200604.
[4] Geng J et al. Voltage-ampere characteristics of YBCO coated conductor under inhomogeneous oscillating magnetic field. Appl Phys Lett 2016;108(26).
[5] Zhong Z, Wu W, Jin Z. Sharp demagnetization of closed-loop HTS coil in first cycle of external AC fields induced by unexpected dynamic resistance. Supercond Sci Technol 2021;34(8).
[6] Pardo E. Dynamic magneto-resistance: turning a nuisance into an essential effect. Supercond Sci Technol 2017;30(6).
[7] Shen B et al. Power dissipation in HTS coated conductor coils under the simultaneous action of AC and DC currents and fields. Supercond Sci Technol 2018;31(7).
[8] Li C et al. Design for a persistent current switch controlled by alternating current magnetic field. IEEE Trans Appl Supercond 2018;28(4):1–5.
[9] Li C, Geng J, Shen B, Ma J, Gawith J, Coombs TA. Investigation on the transformer-rectifier flux pump for high field magnets. IEEE Trans Appl Supercond 2019;29(5):1–5.
[10] Coombs TA. Superconducting flux pumps. J Appl Phys 2019;125(23).
[11] Mataira RC, Ainslie MD, Badcock RA, Bumby CW. Origin of the DC output voltage from a high-Tc superconducting dynamo. Appl Phys Lett 2019;114(16).
[12] Brandt EH, Mikitik GP. Why an AC magnetic field shifts the irreversibility line in type-II superconductors. Phys Rev Lett 2002;89(2).
[13] Grilli F, Morandi A, Silvestri FD, Brambilla R. Dynamic modeling of levitation of a superconducting bulk by coupled H-magnetic field and arbitrary Lagrangian-Eulerian formulations. Supercond Sci Technol 2018;31(12).
[14] Li Q, Yao M, Jiang Z, Bumby CW, Amemiya N. Numerical modeling of dynamic loss in HTS-coated conductors under perpendicular magnetic fields. IEEE Trans Appl Supercond 2018;28(2):1–6.
[15] Oomen MP. Dynamic resistance in a slab-like superconductor with Jc(B) dependence. Supercond Sci Technol 1999;12(6).
[16] Ciszek M, Knoopers HG, Rabbers JJ, ten Haken B, ten Kate HHJ. Angular dependence of the dynamic resistance and its relation to the AC transport current loss in Bi-2223/Ag tape superconductors. Supercond Sci Technol 2002;15(8).
[17] Jiang Z, Hamilton K, Amemiya N, Badcock RA, Bumby CW. Dynamic resistance of a high-Tc superconducting flux pump. Appl Phys Lett 2014;105(11).
[18] Jiang Z, Toyomoto R, Amemiya N, Zhang X, Bumby CW. Dynamic resistance of a high-Tc coated conductor wire in a perpendicular magnetic field at 77 K. Supercond Sci Technol 2017;30(3).
[19] Ainslie M et al. A new benchmark problem for electromagnetic modelling of superconductors: the high-Tc superconducting dynamo. Supercond Sci Technol 2020;33(10).
[20] Ainslie MD, Bumby CW, Jiang Z, Toyomoto R, Amemiya N. Numerical modelling of dynamic resistance in high-temperature superconducting coated-conductor wires. Supercond Sci Technol 2018;31(7).
[21] Ma J et al. Impact of stabilizer layers on the thermal-electromagnetic characteristics of direct current carrying HTS coated conductors under perpendicular AC magnetic fields. IEEE Trans Appl Supercond 2020:1.
[22] Ma J, Geng J, Chan WK, Schwartz J, Coombs T. A temperature-dependent multilayer model for direct current carrying HTS coated-conductors under perpendicular AC magnetic fields. Supercond Sci Technol 2020;33(4).
[23] Brooks JM, Ainslie MD, Jiang Z, Pantoja AE, Badcock RA, Bumby CW. The transient voltage response of ReBCO coated conductors exhibiting dynamic resistance. Supercond Sci Technol 2020;33(3).
[24] Hu D, Ainslie MD, Raine MJ, Hampshire DP, Zou J. Modeling and comparison of in-field critical current density anisotropy in high-temperature superconducting (HTS) coated conductors. IEEE Trans Appl Supercond 2016;26(3):1–6.
[25] Li C et al. Second harmonic in the voltage of dc-carrying YBCO tape under a perpendicular alternating magnetic field. Phys C (Amsterdam, Neth) 2019;564:11–6.
[26] Li C et al. The instantaneous dynamic resistance voltage of DC-carrying REBCO tapes to AC magnetic field. Phys C (Amsterdam, Neth) 2021;583.
[27] Zhang H et al. A full-range formulation for dynamic loss of high-temperature superconductor coated conductors. Supercond Sci Technol 2020;33(5).
[28] Zhang H, Hao C, Xin Y, Mueller M. Demarcation currents and corner field for dynamic resistance of HTS-coated conductors. IEEE Trans Appl Supercond 2020;30(8):1–5.
[29] Hu J et al. Numerical study on dynamic resistance of an HTS switch made of series-connected YBCO stacks. IEEE Trans Appl Supercond 2021;31(5):1–6.
[30] Li C et al. Dynamic resistance of series-connected HTS stacks considering electromagnetic and thermal coupling. IEEE Trans Appl Supercond 2022;32(4):1–5.
[31] Sun Y, Fang J, Sidorov G, Badcock RA, Long NJ, Jiang Z. Dynamic resistance and total loss in a three-tape REBCO stack carrying DC currents in perpendicular AC magnetic fields at 77 K. Supercond Sci Technol 2022;35(3).
[32] Geng J, Brooks JM, Bumby CW, Badcock RA. Time-varying magnetic field induced electric field across a current-transporting type-II superconducting loop: beyond dynamic resistance effect. Supercond Sci Technol 2022;35(2).
[33] Yazdani-Asrami M, Staines M, Sidorov G, Eicher A. Heat transfer and recovery performance enhancement of metal and superconducting tapes under high current pulses for improving fault current-limiting behavior of HTS transformers. Supercond Sci Technol 2020;33(9).

[34] Sun Y et al. Total loss measurement and simulation in a REBCO coated conductor carrying DC current in perpendicular AC magnetic field at various temperatures. Supercond Sci Technol 2021;34(6).
[35] Grilli F. Calculating the full-range dynamic loss of HTS wires in an instant. Supercond Sci Technol 2021;34(2).
[36] Brambilla R, Grilli F, Martini L. Development of an edge-element model for AC loss computation of high-temperature superconductors. Supercond Sci Technol 2007;20(1):16–24.
[37] Jankowski JE. Convective heat transfer model for determining quench recovery of high temperature superconducting YBCO in liquid nitrogen. Doctoral Dissertation Massachusetts Institute of Technology; 2004.
[38] Pi W et al. Investigation on thermal stability of quasi-isotropic superconducting strand stacked by 2 mm wide REBCO tapes and Cu tapes. IEEE Trans Appl Supercond 2020;30(4):1–6.